AN ADAPTIVE CONTROL TECHNOLOGY FOR FLIGHT SAFETY

Luis G. Crespo, Megumi Matsutani and Anuradha M. Annaswamy
***National Institute of Aerospace, ****Massachusetts Institute of Technology**

Keywords: *Adaptive control, flight control, engine control, control verification*

Abstract

This paper focuses on the development, implementation, and verification of an Adaptive Control Technology for Safe Flight (ACTS). We design a controller for an unmanned aerial vehicle and determine the robustness improvements resulting from adaptation by comparing it with a pilot approved non-adaptive controller. The ACTS architecture consists of a nominal controller that provides satisfactory performance under nominal flying conditions, and an adaptive controller that accommodates for anomalous flying conditions resulting from uncertainty, damage and actuator failure. The control surfaces conventionally used for control, as well as the throttle inputs to both engines, are considered controllable inputs. This practice not only alleviates the pilot workload required to compensate for the pitch coupling generated by changes in thrust, but also expands the set of actuator failures for which the plant remains controllable. The adaptive controller accommodates for control saturation and integration windup without allocating the throttle inputs. This feature enables the generation of trust differentials for attitude control. The robustness of the ACTS controller is studied by carrying out control verification studies that evaluate the degradation in closed-loop performance resulting from uncertainties, failures and damages of increasing levels of severity. This analysis indicates the high sensitivity of the closed-loop performance to the speed and range of adaptation and highlights the need for developing control tuning strategies that encompass both theory and practice.

1 Introduction

An adaptive reconfigurable controller autonomously changes the controller gains to maintain satisfactory performance when unforeseen changes in the system dynamics occur. Adaptive control has the potential to improve flight safety, as the loss-of-control is one of the major causes of abnormal flight and fatal accidents. Over the past three decades, adaptive control has been developed extensively and its main performance and robustness properties have been established [7, 1, 5, 4, 8].

In this paper we design a controller for the Generic Transport Model (GTM). The GTM is a dynamically scaled model of a transport aircraft for which NASA Langley has developed a high-fidelity simulink model. This simulation uses non-linear aerodynamic models extracted from wind tunnel data, and considers avionics, sensor dynamics, engine dynamics, atmospheric conditions, sensor noise and biases, telemetry effects, etc. Overall, the open-loop plant has 278 states. Since this model, as the vehicle itself, departs considerably from the Linear Time Invariant (LTI) setting used for control design, it remains to be determined if the improvements in stability, safety, and performance observed in such a setting realize in practice. This paper addresses this question by performing a comparative analysis of the robustness of a pilot-approved non-adaptive controller with its adaptive augmentation. The nominal architecture consists of (i) a longitudinal multivariable controller having the elevator and the throttle inputs to both engines

as controllable inputs and (ii) a lateral/directional multivariable controller having the ailerons and rudders as inputs. A fixed control allocation of the output of the nominal controller precludes using the engines for attitude control. Conversely, the adaptive controller manipulates each of the five controllable inputs independently, therefore, it is solely responsible for generating thrust differentials. Because of the placement of the engines and the orientation of the thrust vector relative to the body axes, changes in thrust create a pitching moment disturbance that must be cancelled by the elevators. Auto throttle designs that only depend on the aircraft velocity rely on the pilot's ability to generate a suitable set of pitch commands to attain the desired cancellation. The ACTS controller pursues this cancellation automatically, thereby it considerably relaxes the pilot's workload.

Control verification studies [2, 3] that evaluate the degradation in closed-loop performance resulting from uncertainties and failures are used to determine the advantages and disadvantages of adaptation. The specific adverse conditions to be considered can be grouped into three categories: aerodynamic uncertainties (e.g., changes in pitch stiffness, roll and yaw damping), structural damages (e.g., situations where the CG move from its nominal location), and actuator failures (e.g., situations where symmetric and asymmetric failures in control surfaces and engines occur). These failures include partial and total losses in control effectiveness as well as locked-in-place control surface deflections and engine out conditions. The requirements considered evaluate (i) the peak structural loading, (ii) the ability of the controller to enable command tracking, (iii) whether the aircraft's state stays within the reliable flight envelope (i.e., region in the state space where the aircraft dynamics are properly modelled and flying is safe), (iv) the handling/riding qualities, and (v) the ability of the controller to track the dynamics of a reference model.

This paper is organized as follows. Sections 2 and 3 presents developments supporting the control design and implementation of the ACTS controller. This is followed by Section 4 where the robustness of the nominal controller and of its adaptive augmentation are compared. Finally, few concluding remarks are made.

2 Control Design

The system's dynamics can be represented as

$$\dot{X} = F(X, \Lambda U) \tag{1}$$

where X is the state, U is the input, and $\Lambda > 0$ is the control effectiveness matrix. For control design purposes, this nonlinear plant is linearized about a trim point (X_0, U_0) satisfying $F(X_0, U_0) = 0$. Deviations from the trim values X_0 and U_0 will be written as lowercase letters in the developments that follow, e.g., $X = X_0 + x_p$ and $U = U_0 + u$. Linearization about the trim point leads to the LTI system

$$\dot{x_p} = A_p x_p + B_p \Lambda u + h(x_p, u) \tag{2}$$

where

$$A_p = \left.\frac{\partial F}{\partial X}\right|_{X_0,\, U_0} \qquad B_p = \left.\frac{\partial F}{\partial U}\right|_{X_0,\, U_0} \tag{3}$$

and $h(x_p, u)$ contains higher order terms. Equation (2) can be written as

$$\dot{x}_p = A_p(\hat{p}) x_p + B_1 \Lambda(\hat{p})(R_s(u) + d) + B_2 \hat{r} \tag{4}$$

where A_p and Λ are unknown matrices that depend on the uncertain parameter vector $\hat{p}$, d is an exogenous disturbance, $\hat{r}$ is the reference command, and $R_s(u)$ is a saturation function that enforces control saturation limits. The nominal value of $\hat{p}$, denoted as $\bar{p}$, corresponds to the case when no uncertainties or failures occur.

The state x consists of angle of attack α, sideslip angle β, aerodynamic speed V, roll rate p, pitch rate q, yaw rate r, longitude x, latitude y, altitude z, and the Euler angles ψ, θ, and ϕ. The control input u consists of the elevators deflection δ_e, the right aileron deflection δ_a, the rudders deflection δ_r, the throttle input to the left engine δ_{thL} and the throttle input to the right engine

δ_{thR}. The reference command r consist of angle of attack-, sideslip-, aerodynamic speed- and roll rate-commands. These four commands, denoted hereafter as α_{cmd}, β_{cmd}, V_{cmd} and p_{cmd} respectively, are generated by the pilot to attain the desired flight maneuver. Both the nominal and adaptive controllers are based on a single trim point design. The procedure used to design them is presented next.

2.1 Nominal Controller

The nominal controller consist of independent controllers for the longitudinal and the lateral/directional dynamics. Both controllers assume a multivariate LQR-PI structure having integral error states for each of the components of the reference command $\hat{r}$. Furthermore, strategies preventing the integration windup caused by input saturation are applied. A fixed control allocation matrix that correlates inputs of the same class is used to determine the ten main plant inputs. As a result, out of these ten inputs only four are independent.

2.1.1 Longitudinal Controller

The plant in the longitudinal axis takes the form

$$\dot{x}_{\text{lon}} = A_{\text{lon}} x_{\text{lon}} + B_{\text{lon}} u_{\text{lon}} \tag{5}$$

where $A_{\text{lon}} \in \mathbb{R}^{3\times 3}$ is the system matrix, $B_{\text{lon}} \in \mathbb{R}^{3\times 2}$ is the input matrix, $x_{\text{lon}} = [\alpha\ q\ V]^\top$ is the state and $u_{\text{lon}} = [\delta_e\ \delta_{th}]^\top$ is the input. In order to closely follow commands in angle of attack and airspeed, the integral error states

$$e_\alpha = \int (\alpha - \alpha_{\text{cmd}})dt \tag{6}$$

$$e_V = \int (V - V_{\text{cmd}})dt \tag{7}$$

are added. This leads to the augmented plant

$$\dot{x}_1 = \begin{bmatrix} A_{\text{lon}} & 0 \\ H_1 & 0 \end{bmatrix} x_1 + \begin{bmatrix} B_{\text{lon}} \\ 0 \end{bmatrix} u_{\text{lon}} + \begin{bmatrix} 0 \\ -I \end{bmatrix} \begin{bmatrix} \alpha_{\text{cmd}} \\ V_{\text{cmd}} \end{bmatrix} \tag{8}$$

where $x_1 = [x_{\text{lon}}^\top\ e_\alpha\ e_V]^\top$. An LQR-PI controller that minimizes

$$J = \int (x^T Q x + u^T R u)dt, \tag{9}$$

where $Q = Q^\top \geq 0$, $R = R^\top > 0$ are weighting matrices, is designed. This leads to

$$\begin{bmatrix} \delta_e \\ \delta_{th} \end{bmatrix} = \begin{bmatrix} K_{\text{lon}}\ K_e \end{bmatrix} x_1 \tag{10}$$

This controller must attain ample stability margins so the inclusion of the low-pass- and anti-aliasing-filters from the sensors and the delay caused by telemetry do not compromise stability.

Due to range saturation, the plant's input is given by

$$R_s(u) = \begin{cases} u & \text{if } u_{min} < u < u_{max}, \\ u_{max} & \text{if } u \geq u_{max}, \\ u_{min} & \text{otherwise} \end{cases} \tag{11}$$

where u is the controller's output, and u_{max} and u_{min} are the saturation limits. The control deficiency caused by this saturation function is given by

$$u_\Delta = R_s(u) - u. \tag{12}$$

Details of an anti-windup technique are presented next. The aim of anti-windup compensation is to modify the dynamics of a control loop during control saturation so that an improved transient behaviour is attained after desaturation. This practice mitigates the chance of having limit cycle oscillations and successive saturation. The anti-windup technique proposed prevents the occurrence of excessively large controller outputs by imposing virtual saturation limits to the integral error state used for feedback. Let $\langle e, \delta \rangle$ denote a strongly coupled pair of an integral error state e and a plant input δ. The anti-windup scheme proposed is governed by the saturation function

$$R_e(e) = \begin{cases} e & \text{if } R_2 \leq e \leq R_1, \\ R_1 & \text{if } R_1 \leq e, \\ R_2 & \text{if } e \leq R_2. \end{cases} \tag{13}$$

where the limits R_1 and R_2 are time-varying functions assuming the smallest value of e for which the plant input is equal to any of its saturation values u_{min} or u_{max}. Note the similarities between

Equation (11) and Equation (13). The integral error state is resetted to the virtual saturation limit when $\dot{e}(t) = 0$ and either $u < u_{min}$ or $u > u_{max}$. Analogous to Equation (12), the error deficiency caused by the anti-windup logic is

$$e_\Delta = R_e(e,\delta) - e. \tag{14}$$

The saturated value of the integral error state $R_e(e)$, not the integral error state itself e, will be used for feedback. Additional details of this technique are available in [3].

In the longitudinal controller case, we apply this strategy to the $\langle e_\alpha, \delta_e \rangle$ pair[1]. As a result, Equation (10) becomes

$$\begin{bmatrix} \delta_e \\ \delta_{th} \end{bmatrix} = \begin{bmatrix} K_{\text{lon}} & K_e \end{bmatrix} \begin{bmatrix} x_{\text{lon}} \\ R_e(e_\alpha) \\ e_V \end{bmatrix} \tag{15}$$

The substitution of u and e with $R_s(u)$ and $R_e(e,\delta)$ into Equation (8) for $u = \delta_e$, and of $e = e_\alpha$ leads to

$$\begin{aligned} \dot{x}_1 = &\begin{bmatrix} A_{\text{lon}} + B_{\text{lon}} K_{\text{lon}} & B_{\text{lon}} K_e \\ H_1 & 0 \end{bmatrix} x_1 + \begin{bmatrix} B_{\text{lon}} \\ 0 \end{bmatrix} \begin{bmatrix} u_{\alpha,\Delta} \\ u_{V,\Delta} \end{bmatrix} \\ &+ \begin{bmatrix} B_{\text{lon}} \\ 0 \end{bmatrix} K_e \begin{bmatrix} e_{\alpha,\Delta} \\ 0 \end{bmatrix} + \begin{bmatrix} 0 \\ -I \end{bmatrix} \begin{bmatrix} \alpha_{\text{cmd}} \\ V_{\text{cmd}} \end{bmatrix} \end{aligned} \tag{16}$$

This Linear Time Varying (LTV) system prescribes the closed-loop longitudinal dynamics with input saturation and integration anti-windup. The boundedness of the resulting system can be established for all initial conditions inside a bounded set. This bounded set extends to the entire state-space when the open-loop plant is stable and there are no unmodeled dynamics.

2.1.2 Lateral/Directional Controller

An LTI model of the corresponding plant is

$$\dot{x}_{\text{lat}} = A_{\text{lat}} x_{\text{lat}} + B_{\text{lat}} u_{\text{lat}} \tag{17}$$

where $A_{\text{lat}} \in \mathbb{R}^{3\times 3}$ is the system matrix, $B_{\text{lat}} \in \mathbb{R}^{3\times 2}$ is the input matrix, $x_{\text{lat}} = [\beta \; p \; r]^\top$ is the state, and $u_{\text{lat}} = [\delta_a \; \delta_r]^\top$ is the input. To enable satisfactory command following, integral error states for sideslip and roll rate, given by

$$e_\beta = \int (\beta - \beta_{\text{cmd}}) dt \tag{18}$$

$$e_p = \int (p - p_{\text{cmd}}) dt \tag{19}$$

are added. The integral error in sideslip was chosen over that of the yaw rate to facilitate the generation of commands for coordinated turns with non-zero bank angles and for cross-wind landing. The augmented plant is given by

$$\dot{x}_2 = \begin{bmatrix} A_{\text{lat}} & 0 \\ H_2 & 0 \end{bmatrix} x_2 + \begin{bmatrix} B_{\text{lat}} \\ 0 \end{bmatrix} u_{\text{lat}} + \begin{bmatrix} 0 \\ -I \end{bmatrix} \begin{bmatrix} \beta_{\text{cmd}} \\ p_{\text{cmd}} \end{bmatrix} \tag{20}$$

where $x_2 = [x_{\text{lat}}^\top \; e_\beta \; e_p]^\top$. A LQR-PI control structure for the lateral controller is adopted. This leads to

$$\begin{bmatrix} \delta_a \\ \delta_r \end{bmatrix} = \begin{bmatrix} K_{\text{lat}} & K_{e_\beta} & K_{e_p} \end{bmatrix} x_2 \tag{21}$$

As before, ample stability margins should be attained to accommodate for the low-pass filters and time delays. The anti-windup technique presented earlier is applied to the $\langle e_\beta, \delta_r \rangle$ and $\langle e_p, \delta_a \rangle$ pairs.

2.1.3 Control Allocation

Equations (10) and (21) along with the three realizations of the anti-windup technique mentioned above, prescribe the input $u_n = [\delta_e \; \delta_a \; \delta_r \; \delta_{th}]^\top$. This input along with a control allocation scheme fully determines the ten control inputs of the aircraft. This relationship can be written as

$$u_{\text{nom}} = G K_n \left[x_{\text{lon}}^\top \; R_e(e_\alpha) \; e_V \; x_{\text{lat}}^\top \; R_e(e_\beta) \; R_e(e_p) \right]^\top, \tag{22}$$

where G is the control allocation matrix, and K_n is the feedback gain. The allocation of u_n enforced by G makes the deflection of the four elevators equal, the thrust of both engines equal, the deflection of both rudders equal, and the deflection of both ailerons equal in magnitude with opposite directions.

[1] The inability of a single LTI model to accurately describe the engine dynamics made the anti-windup logic for $\langle e_V, \delta_{th} \rangle$ ineffective. For this reason, only anti-windup to $\langle e_\alpha, \delta_e \rangle$ is applied.

2.2 Adaptive Controller

The second component of the ACTS is an adaptive controller. This controller generates independent signals for the three main control surfaces as well as for each throttle input.This enables using the engines for attitude control when the rudders fail. An immediate consequence of integrating the engines to the flight control system is the enlargement of the failure set where the vehicle remains controllable. The augmentation of the nominal input leads to

$$u = u_{\text{nom}} + u_{\text{ada}} \tag{23}$$

where u_{ada} is the input corresponding to the adaptive controller. This architecture suits control tuning tasks where u_{nom} is set according to the pilot's input given that sufficiently large stability and performance margins are attained, while u_{ada} is set according to robustness considerations.

The LTI systems used for control design are accurate approximations to the aircraft dynamics as long as such dynamics are weakly coupled. However, for many of the failures and uncertainties that can occur there will be strong coupling, e.g., both left elevators are locked-in-place with a non-zero deflection. In such a case, the adaptive component of the controller, whose underlying dynamic model is coupled, will be active.

2.2.1 *Reference Model*

The reference model is a component of the adaptive controller responsible of driving the output of the adaptive controller. The state of this reference model is the target state of the closed-loop system. In particular, the reference model assumed is prescribed by the linear closed-loop system corresponding to the nominal controller under nominal flying conditions (i.e., $\hat{p} = \bar{p}$). Note that the anti-windup modifications made to the nominal controller are excluded. This leads to

$$\dot{x}_m = \underbrace{[A_p(\bar{p}) + B_1\Lambda(\bar{p})GK_n]}_{A_m} x_m + B_m\hat{r} \tag{24}$$

where $A_m \in \mathbb{R}^{10\times10}$, $B_m \in \mathbb{R}^{10\times3}$, $x_m = [\alpha\ \beta\ V\ p\ q\ r\ e_\alpha\ e_\beta\ e_p\ e_V]^\top$, and $\hat{r} = [\alpha_{\text{cmd}}\ V_{\text{cmd}}\ \beta_{\text{cmd}}\ p_{\text{cmd}}]^\top$. This model will be used to design the adaptive controller. However, this is not the same model we will use to calculate x_m in real time. Details on the process by which the implemented model is derived are provided in Section 3.1.

2.2.2 *Adaptive Law*

The plant to be controlled assumes the LTI representation

$$\dot{x}_p = A_p(\hat{p})x_p + B_1\Lambda(\hat{p})\left(R_s(u) + d\right) + B_2\hat{r} \tag{25}$$

where $A_p \in \mathbb{R}^{10\times10}$, $B_1 \in \mathbb{R}^{10\times5}$, $\Lambda = \text{diag}\{\lambda\} \in \mathbb{R}^{5\times5}$ and $B_2 \in \mathbb{R}^{10\times4}$. The states, inputs, and commands in (25) are

$$\begin{aligned} x_p &= [x_{\text{lon}}^\top\ e_\alpha\ e_V\ x_{\text{lat}}^\top\ e_\beta\ e_p]^\top \\ u &= [\delta_e\ \delta_{th_L}\ \delta_{th_R}\ \delta_a\ \delta_r]^\top \\ \hat{r} &= [\alpha_{\text{cmd}}\ V_{\text{cmd}}\ \beta_{\text{cmd}}\ p_{\text{cmd}}]^\top \end{aligned} \tag{26}$$

while $d \in \mathbb{R}^{5\times1}$ is a vector of input disturbances.

The adaptive input with an anti-windup modification for the pair $\langle e_\alpha, \delta_e\rangle$ is given by

$$u_{\text{ada}} = \theta^\top\omega = \begin{bmatrix}\theta_x^\top\ \theta_d\end{bmatrix}\begin{bmatrix}\hat{x}_p \\ 1\end{bmatrix} \tag{27}$$

where $\theta_x \in \mathbb{R}^{10\times10}$, and $\theta_d \in \mathbb{R}^{1\times10}$ are adaptive parameters, and

$$\hat{x}_p = [x_{\text{lon}}^\top\ f_1(e_\alpha)\ e_V\ x_{\text{lat}}^\top\ e_\beta\ e_p]^\top \tag{28}$$

is the state being fed back. Adaptive laws without the anti-windup modification make f equal to its argument so $\hat{x}_p = x_p$. In the current anti-windup implementation $f_1(e_\alpha)$ is the average value of $R_e(e_\alpha, \delta_e)$ for the four elevators.

The adaptive gains are determined by

$$\dot{\theta} = \text{Proj}\left\{-\Gamma\omega e_u^\top PB_1\text{sign}(\Lambda), \theta_{\max}\right\} \tag{29}$$

$$\dot{\hat{\lambda}} = -\Gamma_\lambda\text{diag}(\kappa)B_1^\top Pe_u \tag{30}$$

$$\dot{e}_\Delta = A_m e_\Delta - B_1\text{diag}\left(\hat{\lambda}\right)\kappa \tag{31}$$

$$\kappa = u_\Delta + (K_{e_\alpha}^\top + \theta_{e_\alpha}^\top)e_{\alpha,\Delta} \tag{32}$$

where $\text{Proj}\{\cdot\}$ is the projection operator [6], $e_u = e - e_\Delta$, $P = P^\top > 0$ satisfies $A_m^\top P + PA_m = -Q$

for a fixed $Q = Q^\top > 0$, $e = x_p - x_m$, and u_Δ is the multivariable version of the input deficiency in Equation (12). While e_Δ is the error caused by saturation in the control inputs and in the integral error state e_α, e_u is the error caused by parametric uncertainties. κ, which along with f_1 constitutes the anti-windup modification, depends on $K_{e_\alpha}^\top$ and $\theta_{e_\alpha}^\top$; which are the column vectors of K_n and θ corresponding to $R_e(e_\alpha, \delta_e)$ and $f_1(e_\alpha)$ respectively. The variables $\Gamma > 0$, $\theta_{\max} > 0$ and $\Gamma_\lambda > 0$ are design parameters that determine the speed and range of adaptation.

This adaptive law makes the plant track the dynamics of the reference model, accommodates for control saturation, and mitigates integral windup in e_α. This architecture requires that all the components of x_p, $e_{\alpha,\Delta}$ and $u_{\alpha,\Delta}$ be accessible. Notice that anti-windup logic is now extended to u as a whole, and not to u_{nom} and u_{ada} independently. However for the $\langle e_V, \delta_{th}\rangle$, $\langle e_\beta, \delta_r\rangle$ and $\langle e_p, \delta_a\rangle$ pairs, anti-windup is only applied to u_{nom}. The strong coupling between β and p makes the anti-windup scheme for $\langle e_\beta, \delta_a\rangle$ and $\langle e_p, \delta_r\rangle$ in the adaptive law ineffective. As before, the inaccurate LTI representation of the engine dynamics with a single LTI model, yield the same outcome for $\langle e_V, \delta_{th}\rangle$. A Lyapunov stability analysis of the resulting closed-loop system demonstrates that for a bounded set of commands, θ, x and e are semi-globally bounded. This result holds under the assumption that the disturbances, time-delays and unmodeled dynamics are small in some sense and that both the plant and the reference model are LTI. The corresponding stability proof is omitted here due to space limitations.

3 Control Implementation

3.1 Reference Model

Due to nonlinearities, the dynamics set by the linear reference model in Equation (24) may differ considerably from those of the actual aircraft. These nonlinearities will undesirably trigger adaptation. Since the primary objective of adaptive control is to compensate for parametric uncertainties -not for nonlinear dynamics- this

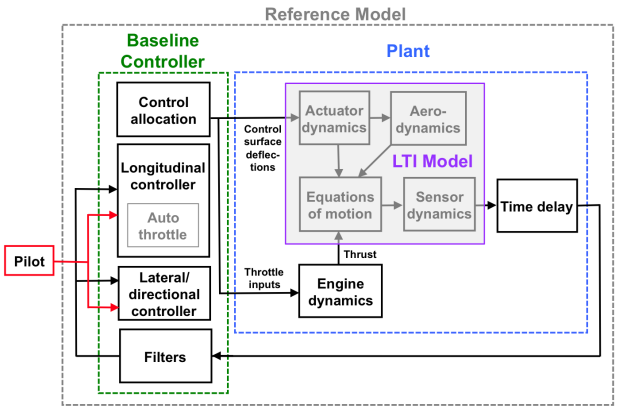

Fig. 1 Reference model.

situation may seriously compromise the stability and performance characteristics of the controller. As such, in this section we examine alternatives that expand the region of the state space where the reference model represents accurately the aircraft dynamics.

One of such choices is to use a full nonlinear reference model. Even though this will directly account for the main nonlinearities, the computational requirements associated with it may be exceedingly high. This complexity results from having to perform a high fidelity simulation in real time as well as to having to verify and validate software and hardware. It is important to determine whether this (or any) reference model prescribes a dynamics that the actual aircraft can realize in practice (even in the case where the vehicle remains controllable and observable after a failure). If physical limitations prevent the aircraft from attaining the dynamics set by the reference model -say due to failure, damage or uncertainty- the controller itself, thereby the plant, may become unstable. This instability, which is triggered by the the controller and not by the plant, can be avoided if a more suitable reference model is designed. The search for an accurate yet simple reference model led us to a system with the following features: (i) the underlying structure of the plant is LTI[2], (ii) there is

[2]There are physical effects for which a single LTI system cannot capture the aircraft dynamics accurately regardless to the proximity of the state to the trim point used for

a nonlinear engine model to accurately describe thrust as a function of the engine's RPMs, (iii) there is uplink time delay between the controller and the plant capturing the effects of telemetry and signal processing, (iv) there is a down link time delay due to the sensor dynamics, (v) there is a bank of low pass filters that mitigate sensor noise, and (vi) there are anti-aliasing filters and command rate limiters as in the actual GTM. The states and inputs of the reference model are $x = [\alpha\ \beta\ V\ p\ q\ r\ x\ y\ z\ \psi\ \theta\ \phi]^\top$ and $u = [\delta_e\ \delta_{th}\ \delta_a\ \delta_r]^\top$. A sketch of the reference model is shown in Figure 1.

3.2 Adaptive Rate

In the LTI framework asymptotic tracking and stability are guaranteed for any adaptive rates satisfying $\Gamma > 0$ and $\Gamma_\lambda > 0$. In such a setting, the larger the adaptive rate the faster the adaptation and the better the performance. This is not the case when nonlinearites and time delays are present. While excessively small adaptive rates diminish the performance advantages resulting from adaptation by practically turning the adaptive controller off, excessively large ones induce high frequency oscillations that can lead to instability. The challenge from the control designer perspective is to balance these two behaviours. The free parameters of the proposed controller were chosen based on the stability and performance characteristics of the system response for several uncertainty realizations and actuator failures.

control design. For instance, the loss in altitude caused by an either positive or negative aileron deflection can not be modelled with a fixed input matrix B. A fixed B matrix leads to a situation where rolling to one side will decrease altitude while rolling to the other one will increase it. Even though this is a second order effect in the coupling between the longitudinal and lateral/directional dynamics, it has the potential to make the target dynamics unrealizable and therefore to drive the system unstable. In order to prevent this from happening, the sign of some of the components of the B_1 matrix in Equations (29)-(31) and in the implemented reference model are switched according to the instantaneous value of the input.

4 Control Verification

4.1 Framework

The robustness of the nominal controller and its adaptive augmentation will be evaluated using the control verification methodology in [2]. The overall objective of this analysis is to determine ranges of uncertainty of $\hat{p}$ in the set $\hat{p}_{min} \leq \hat{p} \leq \hat{p}_{max}$ for which the controller c satisfies a set of closed-loop requirements. The requirements will be satisfied when the constraint set $g(\hat{p}, c) < 0$ is satisfied.

The components of the uncertain parameter vector $\hat{p}$ are as follows. The parameters Λ_{THL}, Λ_{THR}, Λ_{ERO}, Λ_{ERI}, Λ_{ELO}, Λ_{ELI}, Λ_{AL}, Λ_{AR}, Λ_{RU} and Λ_{RD} are the control effectiveness of the main ten inputs. These are the throttle input to the left and right engines, the four elevators, the left and right ailerons; and the upper and lower rudders. These parameters, which are used to describe both the standard loss in control effectiveness and the locked-in-place failure, should be interpreted as follows: if $0 < \Lambda \leq 1$ the actuator will suffer a lose in control effectiveness making the actual plant's input $\Lambda R_s(u + U_0)$ instead of $R_s(u + U_0)$. If $1 \leq \Lambda \leq 0$ the actuator will be locked at the fixed value $u = -\Lambda u_{max}$. Furthermore, $\tau > 0$ is an unknown time delay, $\mu > 0$ is a scaling factor proportional to the amplitude of the command $\hat{r}$ [3], Δ_x is a shift in the CG from its nominal location in the x-direction[4], $C_{m\alpha}$, C_{lp} and C_{nr} are aerodynamic uncertanties in pitch stiffness, roll and yaw

[3] The desired maneuver is composed by a sequence of doublets in α_{cmd}, β_{cmd} and p_{cmd}. When $\mu = 0$ the commands keep the vehicle trimmed at the point used for control design. As μ increases the commands make the vehicle depart from this trim point. The larger the value of μ, the larger such a departure and the larger the effects of the nonlinear dynamics. Note that the vehicle is supposed to return to the trim point in steady state no matter how large μ is. By including μ into $\hat{p}$ we evaluate the degradation in performance caused by inaccuracies in the LTI representation that supports the control design procedure.

[4] The value of Δ_x will be prescribed as a percentage of the mean aerodynamic chord. Besides, its sign is assigned according to the orientation of the body axes, e.g., $\Delta_x = -0.5$ implies an aft shift in the CG location equal to 50% of the mean aerodynamic chord.

damping. The generation of non-zero values for $C_{m\alpha}$ and C_{nr} require that $\Lambda_{ERI} = \Lambda_{ELI} = 0$ and $\Lambda_{RD} = 0$ respectively. The scenario corresponding to $\hat{p} = \bar{p}$ is one in which the amplitude of the pilot commands is moderate ($\mu = 1$), the effectiveness of all actuators is one, there is no additional time delay in the processing and communication of signals, the CG remains at its nominal location and there are no aerodynamic uncertainties.

The design requirements that define a satisfactory closed-loop response are as follows. **Structural loading**: The requirement $g_1 < 0$ ensures that the loading factor caused by the aircraft's acceleration does not exceed the yield stress of the structure.
Command tracking: the requirements $g_i < 0$ for $i = 2,3,4,5$ ensure the aircraft tracks the α, β, p and V commands satisfactorily.
Reliable flight envelope: the requirement $g_6 < 0$ ensures that the vehicle remains within a safe flight envelope throughout the maneuver. Note that a response for which the poor transient response caused by failure makes the vehicle hit the ground will imply the violation of this requirement.
Riding quality/high frequency oscillation: the requirement $g_7 < 0$ bounds the amount of energy in the high-frequency part of the power spectrum of the response. Excessively large adaptation rates induce high frequency oscillations that lead to the violation of this requirement.
Reference tracking: the requirements $g_i < 0$ for $i = 8,9$ bound the offset between the pitch and yaw rates of the plant relative to those of the reference model. Since the command and reference tracking requirements are based on L_2 norms, they take into account the transient response. Details on the functional form of the requirements can be found in [3]. Notice that the dependency of all the components of g on the parameter $\hat{p}$ assume an unknown and implicit functional form. Further notice that evaluating g for a particular realization of $\hat{p}$ requires simulating the closed-loop response and calculating the performance function g.

The controllers to be analyzed are the nominal controller an its adaptive augmentation. These controllers will be denoted as c_{nom} and c_{ada} subsequently. Figure 2 shows the closed-loop response for both controllers when a severe degradation in pitch stiffness and roll damping occurs. The superiority of the adaptive controller is the result of a more aggressive usage of the ailerons and rudders. However, the analysis presented in the next section indicates that this controller is considerably less robust than the baseline controller to other uncertainties.

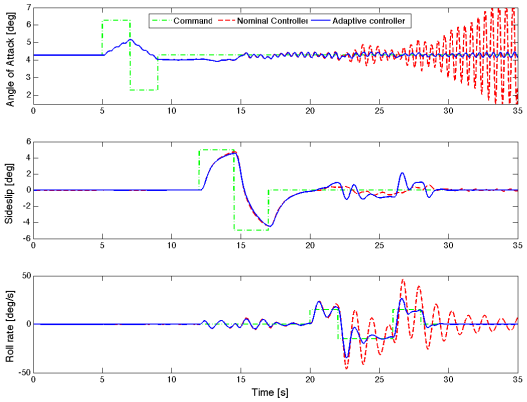

Fig. 2 Responses for c_{nom} and c_{ada}.

In this paper we apply he methodology in [2] to several one-dimensional settings. In this setting, we determine the largest range of $\hat{p}_j$ centered at $\bar{p}_j$ for which $g(\hat{p},c) < 0$ for all set members. This implies that all but one of the components of $\hat{p}$ are fixed at their nominal value while the remaining one is free to vary. The Parametric Safety Margin (PSM) [2] is a measure of the separation between the nominal parameter point $\bar{p}$ and the set in $\hat{p}$-space where the requirements are violated. The PSM corresponding to controller c for the ith requirement in g and the jth uncertain parameter of $\hat{p}$ is

$$\rho_{i,j}(c) = -\text{sign}\{g_i(\bar{p},c)\}\,|\tilde{p}_{i,j} - \bar{p}_j|, \qquad (33)$$

where $\tilde{p}_{i,j}$ is the Critical Parameter Value (CPV). The CPV is given by

$$\tilde{p}_{i,j} = \min_{\hat{p}_j}\left\{|\bar{p}_j - \hat{p}_j|\right\} \qquad (34)$$

subject to $g_i\left(\bar{p} + \delta_j(\hat{p}_j - \bar{p}_j), c\right) = 0$ and $\hat{p}_{min,j} \leq \hat{p}_j \leq \hat{p}_{max,j}$, where δ_j is the Dirac delta. A

$\hat{p}_j$	$\rho(c_{\mathbf{nom}})$
Λ_{THL}	[2.00, 2.00, 2.00, 2.00, 1.87, 1.55, 2.00, 1.92, 1.47]
Λ_{ELO}	[2.00, 2.00, 2.00, 2.00, 1.50, 2.00, 2.00, 2.00, 1.67]
Λ_{AL}	[2.00, 2.00, 2.00, 1.75, 1.27, 1.70, 1.81, 1.81, 1.21]
Λ_{RU}	[2.00, 2.00, 2.00, 2.00, 2.00, 2.00, 2.00, 2.00, 1.30]
τ	[0.07, 0.07, 0.07, 0.07, 0.07, 0.07, 0.07, 0.07, 0.07]
μ	[2.00, 2.00, 2.00, 2.00, 2.00, 1.16, 2.00, 2.00, 2.00]
Δ_x	[0.46, 0.28, 0.46, 0.42, 0.17, 0.12, 0.33, 0.29, 0.42]
C_{lp}	[1.00, 0.96, 1.00, 0.79, 0.87, 0.96, 0.69, 1.00, 0.96]
$C_{m\alpha}$	[1.00, 0.79, 1.00, 0.92, 1.00, 1.00, 0.76, 0.77, 1.00]
C_{nr}	[1.00, 0.90, 0.87, 0.82, 1.00, 1.00, 0.83, 0.92, 0.73]
η	[1,00, 0.95, 1.00, 0.79, 0.87, 0.96, 0.70, 0.95, 0.95]

Table 1 PSMs of c_{nom}.

$\hat{p}_j$	$\left(\frac{\rho(c_{\mathbf{ada}})}{\rho(c_{\mathbf{nom}})}-1\right)\times 100\%$
Λ_{THL}	[0, 0, 0, -1, -2, 0, 0, 0, -1, -62]%
Λ_{ELO}	[0, -19, -23, -23, -4, 0, 0, -18, -36]%
Λ_{AL}	[-52, -63, -83, -84, -67, -45, -49, -49, -63]%
Λ_{RU}	[0, -2, -1, -2, -37, -36, 0, -2, -7]%
τ	[0, 0, 0, -3, -28, 0, 0, -26, 0, -56]%
μ	[0, 0, 0, 0, 0, -11, -13, -9, -88]%
Δ_x	[-4.5, -15, 0, -20, -4, -17, -6, -7, -89]%
C_{lp}	[0, -29, -37, -23, -17, -26, -18, -26, -37]%
$C_{m\alpha}$	[0, -2, -29, -13, 0, 0, -2, 0, -85]%
C_{nr}	[0, -26, -30, -29, -19, -27, -29, -24, -52]%
η	[-2, -6, -10, 12, 3, -7, 26, -6, -5]%

Table 2 Relative PSM change from c_{nom} to c_{ada}.

controller that fails to satisfy a requirement at the nominal parameter point $\bar{p}$ attains a negative PSM. When the PSM takes a positive value the controller satisfies the requirements for the nominal parameter point and its vicinity. The larger the PSM, the larger such a vicinity and the more robust the controller. The PSM is not defined when the CPV does not exist. If this is the case and sign $\{g_i(\bar{p},c)\}<0$, the controller satisfies the ith requirement for all $\hat{p}_j$ realizations in the range of interest. In such a case $\rho_{i,j}(c)=\min\{[\hat{p}_{max,j}-\bar{p}_j, \bar{p}_j-\hat{p}_{min,j}]\}$. In this study the values of $\hat{p}_{min}$ and $\hat{p}_{max}$ are given by $-1\leq\Lambda\leq 1$ for all inputs, $0\leq\tau\leq 0.07$, $0\leq\mu\leq 3$, $-0.5\leq\Delta_x\leq 1$, $0\leq C_{lp}\leq 1$, $0\leq C_{m\alpha}\leq 1$ and $0\leq C_{nr}\leq 1$.

4.2 Results

The PSMs corresponding to the nominal controller for all requirements are listed in Table I[5]. This information enables the identification of the critical parameter and the critical requirement (i.e. the one for which the PSM is the smallest). As expected, the tracking of r is the critical requirement for Λ_{THL}, Λ_{RU}, Λ_{AL} and C_{nr}. The tracking of V on the other hand, degrades the most when the elevator(s) is locked-up. Furthermore, since $\rho(c_{\text{nom}})$ for C_{lp} and $C_{m\alpha}$ assume the smallest value for the $i=7$th requirement, the performance degradation caused by these uncertainties is preceded by unacceptable levels of high frequency oscillation. Table II provides the change in the PSM attained by c_{ada} relative to c_{nom}. While positive values indicate an improvement, negative values indicate a robustness loss. The relative change in the PSM enables determining the advantages and drawbacks of augmenting the nominal controller with an overly aggressive adaptive component. Figure 3 shows $g(\eta,c_{\text{nom}})$ and $g(\eta,c_{\text{ada}})$. The sizable improvements in the tracking of p and V, as well as in the reduction of the high frequency oscillation (i.e. g_4, g_5, g_7) come at the expense of a sudden performance degradation about $\eta=0.88$. Figure 4, where $g(\Lambda_{AL},c_{\text{nom}})$ and $g(\Lambda_{AL},c_{\text{ada}})$ are shown, illustrates the same finite escape time behaviour. At $\Lambda_{AL}=0.05$, c_{ada} becomes unstable making all components of g to blow up. This non-linear phenomenon, which is solely caused by adaptation, occurs abruptly without any lead time for a pilot reaction.

5 Conclusions

This paper proposes and evaluates an adaptive control architecture for safe flight. A comparative analysis of a non-adaptive, pilot approved controller and its adaptive augmentation indicates some advantages and some potential drawbacks of adaptation. While increasing the speed of

[5]The uncertain parameter η implies the combination of aerodynamic uncertainties $C_{lp}=\eta$ and $C_{m\alpha}=0.8\eta$.

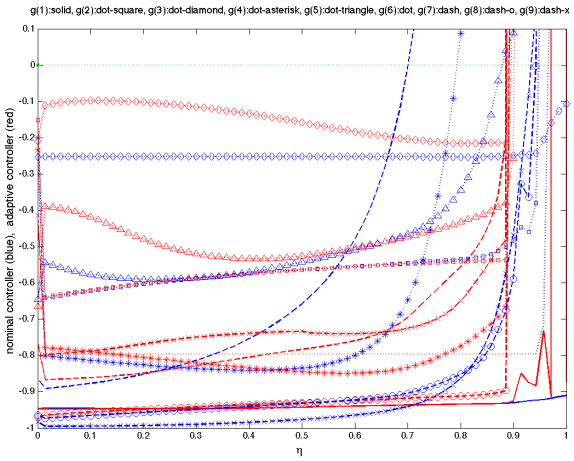

Fig. 3 $g(\eta)$ for c_{nom} and c_{ada}.

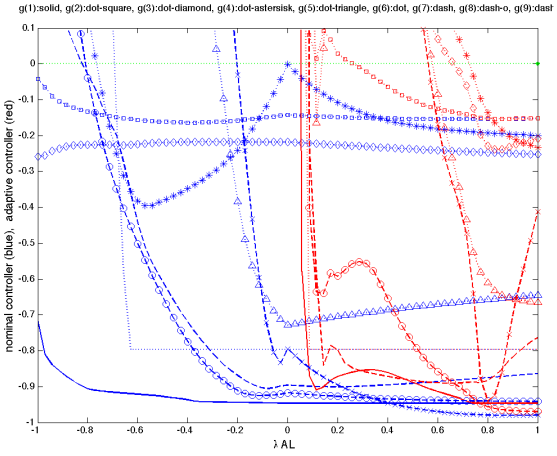

Fig. 4 $g(\Lambda_{AL})$ for c_{nom} and c_{ada}.

adaptation can improve the robustness to aerodynamic uncertainties, it can also make the controller unstable. Trade-offs like this one should drive the process by which the speed and range of adaptation are set. The robustness analysis conducted herein highlights the importance of (i) avoiding the over-tuning of the adaptive control parameters based on localized point uncertainties, (ii) prescribing adaptive rates that are not only sufficiently large to cope with parametric uncertainty but also sufficiently small so nonlinearities, time delays and failures do not trigger instability, (ii) conducting a global control verification study before control validation, and (iv) developing strategies for tuning the control parameters so the overall system robustness is improved.

6 Copyright Statement

The authors confirm that they, and/or their company or organization hold copyright on all of the original material included in this paper. The authors also confirm that they have obtained permission, from the copyright holder of any third party material included in this paper, to publish it as part of their paper. The authors confirm that they give permission, or have obtained permission from the copyright holder of this paper, for the publication and distribution of this paper as part of the ICAS2010 proceedings or as individual off-prints from the proceedings.

References

[1] Karl J. Astrom and Bjorn Wittenmark. *Adaptive Control*. Addison-Wesley, Reading, MA, 2nd edition, 1994.

[2] L. G. Crespo, S. P. Kenny, and D. P. Giesy. A computational framework to control verification and robustness analysis. In *NASA TP 2010-216189*, pages 1–38, NASA Langley Research Center, Hampton, VA, 2010.

[3] Luis G. Crespo, M. Matsutani, and Anuradha M. Annaswamy. Design and verification of an adaptive controller for the generic transport model. In *Proceedings of AIAA Guidance, Navigation, and Control Conference and Exhibit*, Chicago, IL, USA, 2009. AIAA 2009-5618.

[4] Petros A. Ioannou and Jing Sun. *Robust Adaptive Control*. Prentice Hall, Upper Saddle River, NJ, 1996.

[5] Y. D. Landau. *Adaptive Control: The model reference approach*. Marcel Dekker, New York: NY, 1979.

[6] Eugene Lavretsky. The projection operator. Personal Notes, 2006.

[7] Kumpati S. Narendra and Anuradha M. Annaswamy. *Stable Adaptive Systems*. Prentice Hall, Englewoods Cliffs, NJ, 1989.

[8] Shankar S. Sastry and Marc Bodson. *Adaptive Control: Stability, Convergence, and Robustness*. Prentice Hall, Englewood Cliffs, NJ, 1989.